JOHNSON-COOK FAILURE MODEL FOR ADDITIVELY MANUFACTURED 304L STAINLESS STEEL PARTS

H.A. Haffner[1], M. Rangapuram[1], S.K. Dasari[1], S.P. Isanaka[1], K. Chandrashekhara[1], M.F. Buchely[2], and J.W. Newkirk[2]

[1]Department of Mechanical and Aerospace Engineering
[2]Department of Materials Science and Engineering
Missouri University of Science and Technology, Rolla, MO 65409

Abstract

Laser powder bed fusion (LPBF) process is a type of additive manufacturing technique which uses a powder bed to form complex metal parts in a layer-by-layer process. This study aims to understand the damage initiation in the parts manufactured by LPBF process using 304L stainless steel powder, which is widely used in numerous applications. The tensile specimens were manufactured using 304LSS powder through LPBF. Tensile specimens with varying notches were tested to calibrate the parameters of the constitutive Johnson-Cook failure model. To obtain the strength parameters, the tensile tests were performed at different temperatures and strain-rates. The material model developed was used in numerical simulation of the tensile tests and compared with the experimental results.

Keywords: Johnson-Cook damage model; finite element simulation; laser powder bed fusion; 304L stainless steel

1. Introduction

Additive manufacturing (AM) has garnered awareness in recent years given its inherent design versatility and ability to fabricate complex parts for the automotive, aerospace, and medical industries in a timely manner[1]–[3]. The AM technology can be grouped into 7 categories, which include binder jetting, sheet lamination, direct energy deposition (DED), laser powder bed fusion (LPBF), material jetting (MJ), material extrusion (ME), and vat photopolymerization[4], [5]. Among the available AM technologies, the LPBF and DED has gained more attention given to the accuracy, precision to manufacture complex geometry. However, some drawbacks associated with DED include the larger volumes of inert gases and lower resolution of manufactured part compared to LPBF [5]. The LPBF method has proven to manufacture dense parts of 99.8% relative density with remarkably fine structure, high degree of accuracy and good resolutions[6]–[8]. The LPBF process is a layer-by-layer process that utilizes high power laser to melt and solidify respective layers with powder particles in the range of 15-53μm. Studies have shown that the build parameters in LPBF process significantly influences the structure, invariably, the properties of the final part manufactured[9], [10].

The understanding of the flow stress behavior of material through modeling is a function of various parameters not limited to the strain rate, temperature, loading and the structural features of the material [11], [12]. Generally, constitutive damage models are utilized in the study of the

mass flow behavior using finite element analysis, given its robust material model and advantage over other numerical methods in simulation[13], [14]. Several damage models that have been incorporated into numerical codes, some of which include, the modified Cockcroft-Latham fracture criterion[15], the Wilkins fracture model[16], the Johnson-Cook damage model[17]. However, the Johnson-Cook material and damage model has been substantially utilized in industrial setting, using finite element simulation, to model flow behavior of materials at high strain rates and temperatures[18]. The aim of this current work encapsulates obtaining the Johnson-Cook (JC) damage model parameters for additively manufactured 304L stainless steel. To achieve this, three sample configurations, with no notch and two different notch sizes, were fabricated and tested with 0.001 strain rate. Finite element analysis was used to obtain the stress triaxialities for the three configurations and incorporated to obtain damage model parameters. The comparison between the developed model and experimentation from tensile testing was evaluated.

2. **Materials and Methodology**

2.1 Johnson-Cook Damage Model

The Johnson-Cook damage model is a constitutive model used to study the flow behavior of material and it is a function of the material's strain rate, stress triaxiality, fracture strain and temperature[11], [14], [18]. The Johnson-Cook damage model can be expressed as follows:

$$\varepsilon_{eq} = (D_1 + D_2 exp(- D_3\sigma^*))(1+ D_4 ln\ \dot{\varepsilon}_*)(1+ D_5\ T^*) \tag{1}$$

Where D_1, D_2, D_3, D_4, D_5 are failure parameters, ε_{eq} is the equivalent strain to failure, $\dot{\varepsilon}_*$ is the non-dimensional strain rate, σ^* is the stress triaxiality and T^* is the homologous temperature given by

$$T^* = \frac{T- T_r}{T_m- T_r} \tag{2}$$

The failure parameters are determined experimentally and is outlined in section 3.

2.2 Materials and AM Parts

For the present study gas atomized 304L stainless steel material with powder range of 15μm - 53μm was used to fabricate the test coupons for the Johnson-Cook failure model parameters. Table 1 delineates the elemental composition of the material in weight percentage. The fabrication involved the use of the Renishaw AM250 with an effective build volume of 250x250x365mm³.

Table 1. Elemental composition of 304L SS Powder

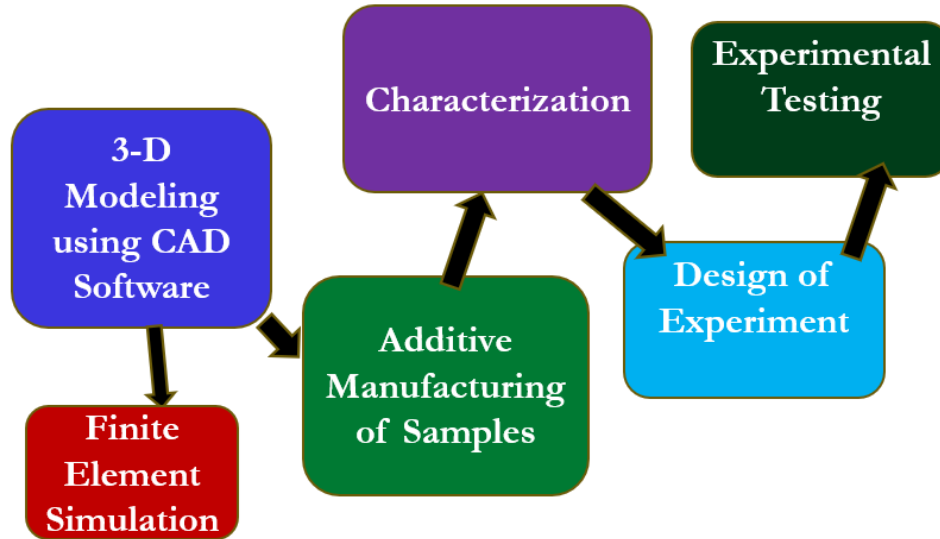| Element	C	N	Si	Ni	Cr	Mn	Cu	Mo	P
Wt (%)	0.025	0.070	0.015	7.900	17.700	1.750	0.840	0.320	0.030

Figure 1. Flow chart depicting methodology for the study.

3. Experimental Testing

3.1 Testing of Unnotched and Notched Samples

The part fabricated for this study included 2mm thick tensile samples printed in the XY-direction and Z-direction with three different notch configurations which include the unnotched, the notched radius of 4.8mm, and the notched radius of 2.0mm. The ASTM-E8 standard was used in the fabrication of these samples.
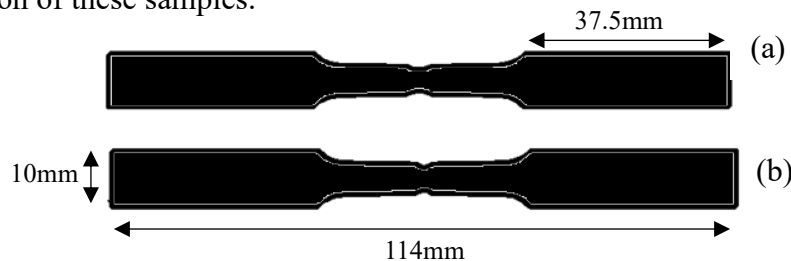

Figure 2: Tensile coupons with (a) notch radius of 4.8mm (b) notch radius of 2.0mm

Using an MTS systems equipment, tensile tests was done on the 2.0mm notched, 4.8mm notched and the un-notched sample. Figure 3 shows the tensile test equipment used for the tensile test.
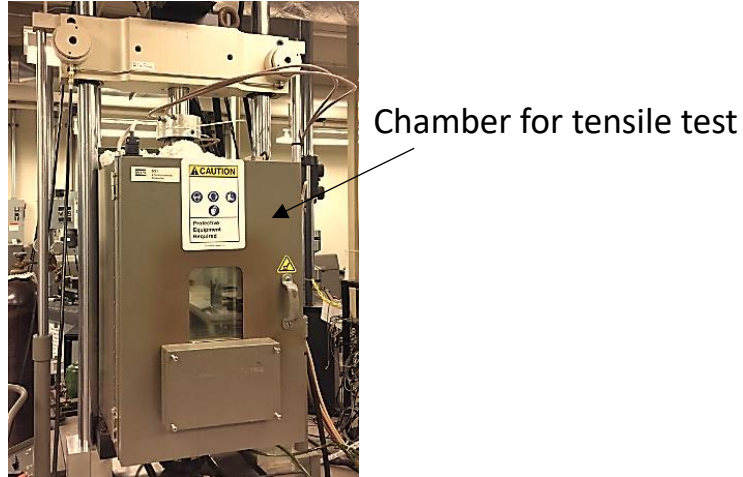
Figure 3: MTS frame tensile test equipment

3.2 Design of Experiment

One-way experimental design with the incorporation of a randomized complete block design (RCB) was used for this study in which the variable factor is the notch radius. Table 2 shows the experimental design set-up using strain rate and reference temperature of $0.001s^{-1}$ and $25°C$ respectively to obtain a 3-treatment combination design. For each treatment combination, three replications were done.

Table 2. Experimental design

Notch configuration	Notch radius of 4.8mm	Notch radius of 2.0mm	Unnotched
Strain rate (s^{-1})	0.001	0.001	0.001
Temperature $(°C)$	25	25	25

4. Results and Discussion

4.1 Finite Element Model

For finite element simulations, ABAQUS software was used to simulate the model for verification study of the JC damage parameters obtained from the tests. A linear quadrilateral element of type CPS4R was used for the meshing. The strength parameters used in this study for 304L SS is the same as reported in our previous study [19] and is shown in Table 3. The simulation involved subjecting one end to fixed boundary condition and the other end to displacement along the y-axis.

Table 3. Johnson-Cook strength model parameters obtained for 304L SS

Parameters	XY-direction	Z-direction
A (MPa)	516.45	491.83
B (MPa)	812.39	571.40
n	0.7042	0.6422
C	0.0117	0.0118
m	0.7383	0.7727
$\dot{\varepsilon}_0$ (s^{-1})	0.001	0.001

4.2 Obtaining D1, D2 and D3 Parameters

To obtain the values of D_1, D_2, and D_3 for the JC damage model the fracture strain was plotted against the stress triaxiality of the 3 different notch configurations[14] as shown in Figure 4. The plot was curve-fitted to Equation (3) to obtain the values of D_1, D_2 and D_3. Table 4 shows the summary of the results for D_1, D_2, and D_3 in both directions.
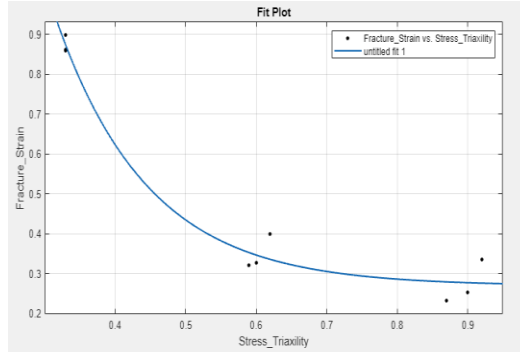

Figure 4: Plot of fracture strain vs stress triaxiality for 3 different notch configurations.

Curve-fit equation:
$$f(x) = a \times \exp(-b \times x) + c \tag{3}$$

Table 4. D_1, D_2 and D_3 parameters for XY-direction and Z-direction.

Parameters	XY-direction	Z-direction
D_1	0.2697	0.2232
D_2	7.4534	6.7951
D_3	7.6160	7.1087

4.3 Obtaining D4 and D5 Parameters

D4 and D5 parameters of the JC damage model are considered the strain dependent and temperature dependent constants. Figure 5 and Figure 6 shows the obtained results for D4 and D5 respectively for XY-direction and Z-direction. To obtain D4, the fracture strain was calculated from the reference temperature, 25°C, and strain rates of 0.1/s, 0.01/s, and 0.001/s. D5 was obtained from the fracture strain calculated at a reference strain rate of 0.001/s and temperatures of 25°C, 125°C, and 250°C. Table 5 shows the summary of the results for D4 and D5 in both directions.
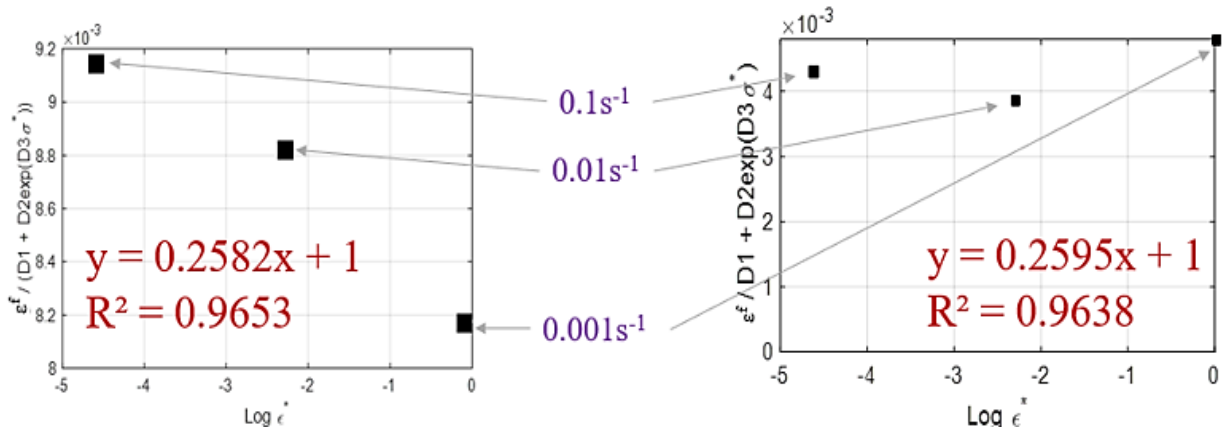

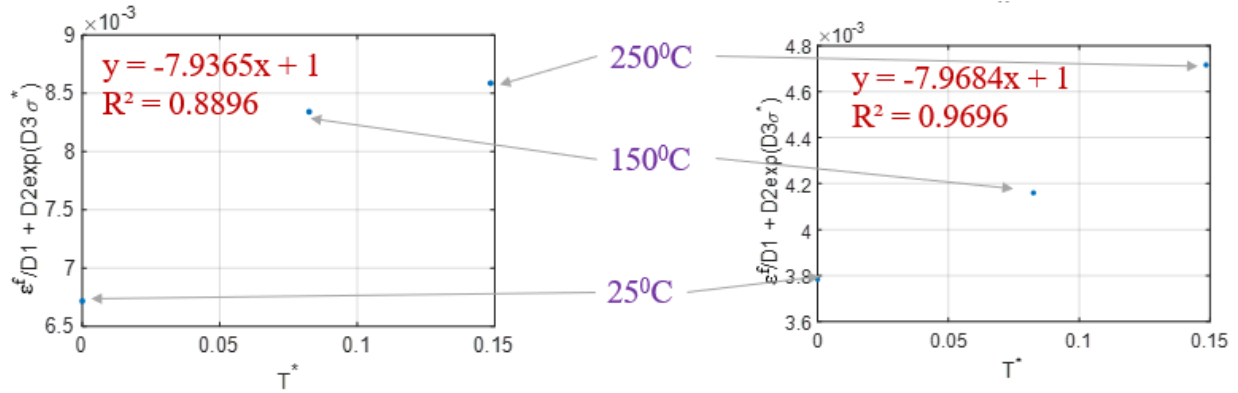Figure 5. Plot showing the D_4, strain dependent parameter for XY-direction and Z-direction.

Figure 6. Plot showing the D_5, temperature dependent parameter for XY-direction and Z-direction.

Table 5. D_4 and D_5 parameters for XY-direction and Z-direction.

Parameters	XY-direction	Z-direction
D_4	0.2582	0.2595
D_5	-7.9365	-7.9684

4.3 Finite Element Modeling and Experimental Results Comparison

Explicit/dynamic simulations using ABAQUS was performed to obtain the finite element model that was compared with the experimental obtained results. Figure 7 shows both experimental and simulation complement each other with less than 2% difference in obtained dimensions which indicates the damage parameters are a good fit.
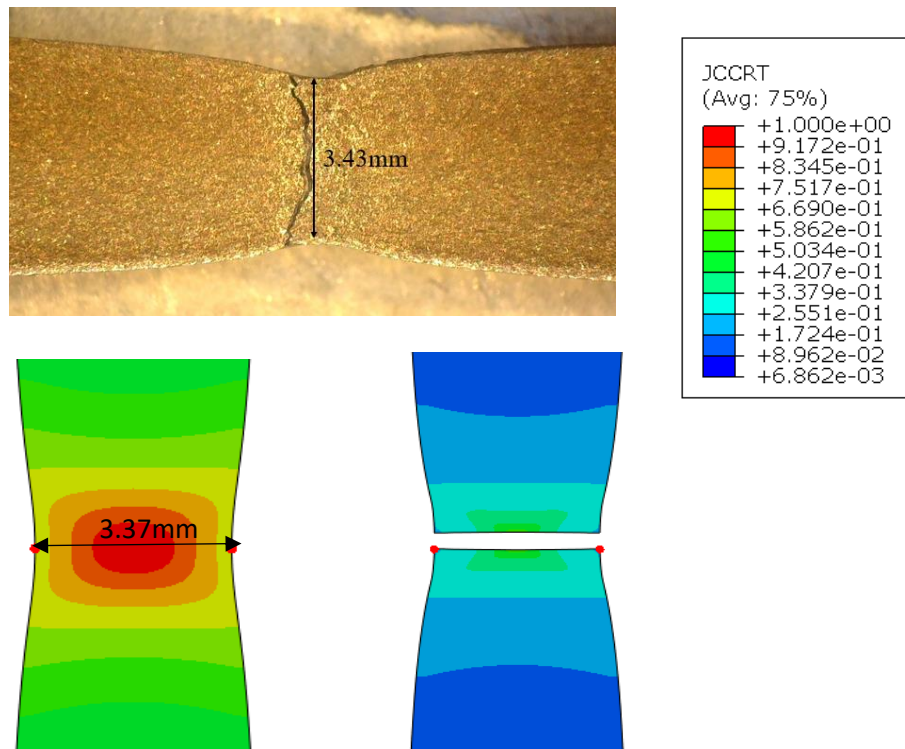

Figure 7. Comparison between the experimental and numerical simulation.

5. Conclusion

Johnson-Cook (JC) damage parameters were obtained for 304L stainless steel for the XY-direction and Z-direction. The JC parameters 304L SS were determined experimentally and incorporated in ABAQUS to simulate the tensile test model. The result was compared with experimental results and the comparison showed that the results are close between the experimental and simulation with a difference within 2%.

6. Reference

[1]   L. S. Bertol, W. K. Júnior, F. P. da Silva, and C. Aumund-Kopp, "Medical design: Direct metal laser sintering of Ti-6Al-4V," *Materials & Design*, vol. 31, no. 8, pp. 3982–3988, 2010, doi: 10.1016/j.matdes.2010.02.050.

[2]   A. Takaichi Suyalatu, T. Nakamoto, N. Joko, N. Nomura, Y. Tsutsumi, S. Migita, H. Doi, S. Kurosu, A. Chiba, N. Wakabayashi, Y. Igarashi and T. Hanawa "Microstructures and mechanical properties of Co-29Cr-6Mo alloy fabricated by selective laser melting process for dental applications," *Journal of the Mechanical Behavior of Biomedical Materials*, vol. 21, pp. 67–76, 2013, doi: 10.1016/j.jmbbm.2013.01.021.

[3]   B. Qian, K. Saeidi, L. Kvetková, F. Lofaj, C. Xiao, and Z. Shen, "Defects-tolerant Co-Cr-Mo dental alloys prepared by selective laser melting," *Dental Materials*, vol. 31, no. 12, pp. 1435–1444, 2015, doi: 10.1016/j.dental.2015.09.003.

[4]   J. J. Beaman, D. L. Bourell, C. C. Seepersad, and D. Kovar, "Additive Manufacturing Review: Early Past to Current Practice," *Journal of Manufacturing Science and Engineering, Transactions of the ASME*, vol. 142, no. 11, pp. 1–20, 2020, doi: 10.1115/1.4048193.

[5]   A. Shah, R. Aliyev, H. Zeidler, and S. Krinke, "A Review of the Recent Developments and Challenges in Wire Arc Additive Manufacturing (WAAM) Process," *Journal of Manufacturing and Materials Processing*, vol. 7, no. 3, pp. 1-30, 2023, doi: 10.3390/jmmp7030097.

[6]   K. Saeidi, D.L. Zapata, F. Lofaj, L. Kvetkova, J. Olsen, Z. Shen, and F. Akhtar "Ultra-high strength martensitic 420 stainless steel with high ductility," *Additive Manufacturing*, vol. 29, pp. 1-6, 2019, doi: 10.1016/j.addma.2019.100803.

[7]   T. Ron, A. Shirizly, and E. Aghion, "Additive Manufacturing Technologies of High Entropy Alloys (HEA): Review and Prospects," *Materials*, vol. 16, no. 6, pp. 1-31, 2023, doi: 10.3390/ma16062454.

[8]   K. Li, T. Yang, N. Gong, J. Wu, X. Wu, D.Z. Zhang, and L. E. Murr, "Additive manufacturing of ultra-high strength steels: A review," *Journal of Alloys and Compounds*, vol. 965, no. July, pp. 1-33, 2023, doi: 10.1016/j.jallcom.2023.171390.

[9]   E. Liverani, S. Toschi, L. Ceschini, and A. Fortunato, "Effect of selective laser melting (SLM) process parameters on microstructure and mechanical properties of 316L austenitic stainless steel," *Journal of Materials Processing Technology*, vol. 249, no. November 2016, pp. 255–263, 2017, doi: 10.1016/j.jmatprotec.2017.05.042.

[10] O. Fashanu, M.F. Buchely, M. Spratt, J. W. Newkirk, K. Chandrashekhara, H. Misak and M. Walker, "Effect of SLM build parameters on the compressive properties of 304L stainless steel," *Journal of Manufacturing and Materials Processing*, vol. 3, no. 2, pp. 1-15, 2019, doi: 10.3390/jmmp3020043.

[11] G. H. Majzoobi and F. R. Dehgolan, "Determination of the constants of damage models," *Procedia Eng*, vol. 10, pp. 764–773, 2011, doi: 10.1016/j.proeng.2011.04.127.

[12] J. Wang, W. Guo, J. Guo, Z. Wang, and S. Lu, "The Effects of Stress Triaxiality, Temperature and Strain Rate on the Fracture Characteristics of a Nickel-Base Superalloy," *Journal of Material Engineering and Performance*, vol. 25, no. 5, pp. 2043–2052, 2016, doi: 10.1007/s11665-016-2049-9.

[13] V. T. S. Ganguly, X. Wang, K. Chandrashekhara, M.F. Buchely, S. Lekakh, R.J. O'Malley, A. Kumar, "Modeling and simulation of mass flow during hot rolling low carbon steel I-beam," *Journal of Manufacturing Process*, vol. 64, pp. 285–293, 2021.

[14] M. F. Buchely, X. Wang, D. C. Van Aken, R. J. O'Malley, S. Lekakh, and K. Chandrashekhara, "The Use of Genetic Algorithms to Calibrate Johnson-Cook Strength and Failure Parameters of AISI/SAE 1018 Steel," *Journal of Engineering Materials and Technology, Transactions of the ASME*, vol. 141, no. 2, pp. 1–12, 2019, doi: 10.1115/1.4042382.

[15] M. Terhorst, A. Feuerhack, D. Trauth, and F. Klocke, "Extension of the normalized Cockcroft and Latham criterion with temperature-dependent critical damage values for predicting chevron cracks in solid forward extrusion," *International Journal of Material Forming*, vol. 9, no. 4, pp. 449–456, 2016, doi: 10.1007/s12289-015-1231-1.

[16] M. L. Wilkins, R. D. Streit, and J. E. Reaugh, "Cumulative-Strain-Damage model of ductile fracture: Simulation and prediction of engineering fracture tests," *Lawrence Livermore National Laboratory*, pp. 1–68, 1980.

[17] G. R. Johnson and W. H. Cook, "Fracture characteristics of three metals subjected to various strains, strain rates, temperatures and pressures," *Engineering Fracture Mechanics*, vol. 21, no. 1, pp. 31–48, 1985, doi: 10.1016/0013-7944(85)90052-9.

[18] M. Murugesan and D. W. Jung, "Johnson-Cook material and failure model parameters estimation of AISI-1045 medium carbon steel for metal forming applications," *Materials*, vol. 12, no. 4, pp. 1-18, 2019, doi: 10.3390/ma12040609.

[19] M. Rangapuram, S. K. Dasari, S. P. Isanaka, M.F. Buchely, J. W. Newkirk, and K. Chandrashekhara, "Calibration of the Johnson-Cook material model for additively manufactured 304L SS parts: modeling and experiments," Proceedings of the 33rd Annual International Solid Freeform Fabrication (SFF) Symposium, Austin, TX, pp. 1-11, July 25-27, 2022.